

## XI-12.

## Acoustoelectric Phenomena in Tellurium

G. QUENTIN and J. M. THUILLIER

*Laboratoire de Physique, Ecole Normale Supérieure, Paris 5,  
France*

We observed in Tellurium current saturation and current oscillations; the former is related to the existence of a high field domain trapped near one end, the latter with the propagation of such a domain. A study of the anisotropy of these phenomena is reported. We propose a theoretical explanation which is a generalisation of White's theory of amplification, including the possibility of off-axis waves amplification. This explanation gives a good account of the critical drift velocity, the domain's velocity, the direction of transverse acoustoelectric field and that of the normal to "tilted" domains.

### § 1. Introduction

Tellurium belongs to the same crystal class as  $\alpha$  quartz (32). It is one of the most highly piezoelectric materials; the piezoelectric constant  $d_{11}$  and the electromechanical coupling constant<sup>1)</sup> for [100] direction have the following values:

$$d_{11} = 3.7 \times 10^{-11} \text{ CN}^{-1}, K_1 = \sqrt{d_{11}^2 / \epsilon_1 s_{11}} = .35.$$

We did not achieve the measurements of the second piezoelectric constant  $d_{14}$  at the present time because of experimental difficulties. Ultrasonic amplification was achieved by Ishiguro *et al.*<sup>2)</sup> with a maximum gain of 33 dB/cm at 45 MHz.

All the experiments described in this paper were made at 77°K where tellurium is a  $p$ -type extrinsic semiconductor.

When the drift velocity of holes exceeds sound velocity we observe the build up of a high field domain which, for some samples travels from anode to cathode, and for others remains "trapped" near one end.

The first experiments<sup>3,4)</sup> were made with samples, the greatest dimension of which was along [100] axis. Here we shall report experiments with current along [010] and [001] and show the existence of off-axis acoustoelectric fields and the motion of a high field domain which is not perpendicular to the  $dc$  current. A theoretical explanation will be proposed.

### § 2. Off-Axis Wave Amplification

In the following the symbols have their usual meaning. Our equations are similar to those of Hutson and White<sup>5)</sup> and White<sup>6)</sup>, but off-axis propagation is taken into account. The basic equations are the mechanical wave equations, the

Maxwell equations and the piezoelectric equations of state:

$$\vec{T} = c \vec{S} - e \vec{E} \quad (1)$$

$$\vec{D} = e \vec{S} + \epsilon \vec{E}. \quad (2)$$

The current density in an extrinsic semiconductor, neglecting trapping, is

$$\vec{J} = q \vec{\mu} (n + n_s) \vec{E} + q \vec{\mathcal{D}} \cdot \vec{\nabla} n_s. \quad (3)$$

We now assume a plane wave time and space dependence

$$\vec{u} = \vec{u}_s \exp j(\vec{k} \cdot \vec{r} - \omega t), \quad (4)$$

$$\vec{E} = \vec{E}_0 + \vec{E}_s \exp j(\vec{k} \cdot \vec{r} - \omega t) \dots \quad (5)$$

and limit us to the linear theory; thus we neglect the quadratic term  $n_s \vec{E}_s$  in  $\vec{J}$ .

The equation of charge continuity

$$\vec{\nabla} \cdot \vec{J} = -\delta Q / \delta t = -q \delta n_s / \delta t = -\delta(\vec{\nabla} \cdot \vec{D}) / \delta t, \quad (6)$$

can be written

$$\vec{k} \cdot \vec{I}_s = 0, \quad (7)$$

where  $I_s$  is the  $ac$  part of the current

$$\vec{I}_s = \vec{\sigma} \vec{E}_s - j(\vec{k} \cdot \vec{D}_s) \vec{\mu} \vec{E}_0 + (\vec{k} \cdot \vec{D}_s) \vec{\mathcal{D}} \vec{k} - j\omega \vec{D}_s.$$

It is now useful to split the acoustoelectric field  $\vec{E}_s$  into two components  $\vec{E}_{s||}$  along the  $\vec{k}$  vector and  $\vec{E}_{s\perp}$ . The Maxwell equations and (7) lead to

$$\vec{E}_{s\perp} = j\omega \frac{\mu_0}{k^2} \vec{I}_s.$$

Hutson and White have shown, in the case of propagation along a principal axis, that if we neglect  $\vec{E}_{s\perp}$  the error introduced in the final re-

sult is of the order of  $V^2/c^2$  where  $c$  is the phase velocity of light and  $\vec{V}=\omega\vec{k}/k^2$  (velocity of sound in direction  $\vec{k}$ ). With this assumption we obtain

$$\vec{T}=\vec{c'}\vec{S} \quad (8)$$

where

$$\vec{c'}\vec{S}=\vec{c}\vec{S}-e\vec{k}(\vec{k}\cdot\vec{e}\vec{S}) \times \left[ \frac{\vec{k}\cdot\vec{\sigma}\vec{k}}{\vec{j}\vec{k}\cdot\vec{\mu}\vec{E}_0-\vec{k}\cdot\vec{\mathcal{D}}\vec{k}+j\omega} -\vec{k}\cdot\vec{\varepsilon}\vec{k} \right]^{-1}. \quad (9)$$

The index  $i$  corresponds to the three different acoustic waves propagating along  $(\theta, \varphi)$ ,  $v_i$  is the velocity of sound neglecting piezoelectric correction,  $K_i$  is the electromechanical coupling constant of the acoustic wave. The properties of the tellurium samples used allow other simplifications.

With  $\sigma=1\Omega^{-1}\text{cm}^{-1}$  and  $\mu=5000\text{cm}^2/\text{V sec}$ ,  $\omega_e\sim 4\times 10^{11}\text{c/sec}$  and  $\omega_D\sim 1.7\times 10^9\text{c/sec}$  and if  $|\gamma|= \left| 1+\frac{\mu E_0 \cos \beta}{v_i} \right| < 10$  where  $\beta$  is the angle between  $\vec{k}$  and  $\vec{E}_0$ , the amplification coefficient  $\alpha$  and the modified sound velocity  $V^*$  are given by

$$\alpha=\frac{-K_i^2}{2v_i\omega_e}\left(\frac{\omega}{1+\omega^2/\omega_e\omega_D}\right)^2\left(1+\frac{\mu E_0 \cos \beta}{v_i}\right), \quad (10)$$

$$V^*=V\left[1+\frac{K^2}{2}\left(\frac{\gamma^2\omega^2}{\omega_e^2}+\frac{\omega^2}{\omega_e\omega_D}+\frac{\omega^4}{\omega_e^2\omega_D^2}\right)\times\left(1+\frac{\omega^2}{\omega_e\omega_D}\right)^{-2}\right]. \quad (11)$$

### § 3. Application to Tellurium

From the expression of the modified elastic constants  $\vec{c'}$  given by (9) we can easily deduce the values of the phase velocity  $\omega/k$  of the acoustic wave. Such a computation was carried out for tellurium with the following approximations: the mobility  $\vec{\mu}$  and the dielectric permittivity  $\vec{\varepsilon}$  are assumed isotropic. The direction is given in spherical coordinates,  $\theta$  being the angle between it and the [001] axis. We obtain the following expression for the phase velocity  $\omega/k$  in direction  $(\theta, \varphi)$ ;

$$\frac{\omega}{k}=v_i(\theta, \varphi)\sqrt{1+K_i^2(\theta, \varphi)\left[1+j\frac{\omega_e}{\omega}\left(1+\frac{\vec{\mu}\vec{k}\cdot\vec{E}_0}{kv_i(\theta, \varphi)}+j\frac{\omega}{\omega_D}\right)^{-1}\right]^{-1}}$$

From (10) one can deduce  $\alpha$  versus direction and value of the applied field  $\vec{E}_0$ . Unfortunately the value of the piezoelectric stress constants  $e_{11}$  and  $e_{14}$  are not known. Here we have assumed that  $2|e_{14}|<|e_{11}|$ .

The velocity of sound in tellurium is highly anisotropic and varies from 1.02 to  $3.82\times 10^5\text{cm/sec}$ . The maximum value of  $K_i(\theta, \varphi)$  lies in a direction very close to that of the minimum value of  $v_i(\theta, \varphi)$  and the angular variations of  $K_i$  are very great. If the angle  $\gamma$  between the electric field and the direction  $\vec{k}_0$  of a minimum value of  $\vec{v}_i$  is not too large it can be expected that maximum amplification occurs along  $\vec{k}_0$ . This will be discussed later for each type of sample.

### § 4. Experimental Results and Discussion

#### a) Type III samples (axis along [001])

The saturation of current was first observed by Kanai<sup>8)</sup>. He interpreted it as a result of holes'

Table I. Sample properties.

Sample	$\sigma$ $\text{cm}^{-1}\Omega^{-1}$	$\mu$ $\text{cm}^2/\text{V sec}$	$n$ $10^{15}/\text{cm}^3$	$\mu_H Ec$ $10^5\text{cm/sec}$	$v_d$ $10^5\text{cm/sec}$
$\times$ Kanai Ref. 8	9.6	3370	17.8	4.05	
III 11	2.25	8000	1.7	4.1 to 4.4	
III 44	.41	3200	.8	4.5 to 5	
II 46	.34	2030	1.1	1.10	
II 47	.76	3180	1.5	1.34	
II 52	.45	4700	.6	1.25	
I 29	1.85	4500	2.6	2.12	
I 33	1.4	4550	1.9	2.22	
I 35	.61	2650	1.4		1.3 to 1.6
I 49	1.31	4800	1.7		1.6

heating. We have carried out similar measurements and the results are given in Table I. Along [001] no piezoelectrically coupled wave can propagate. The velocities of sound are 2.35 and 3.51  $\times 10^5$  cm/sec. The calculation of off-axis waves maximum amplification direction is rather complicated because of the large variations of  $\cos \beta$  in formula (10) in the range where  $K_i^2/v_i$  is maximum, but this interpretation may probably explain that we observed a kink for values of drift velocity greater than any sound velocity.

The potential distribution has been studied in sample III 44 and does not show any formation of high field domain.

b) Type II samples (axis along [010])

The axis of the crystal makes a small angle with a direction  $\vec{k}_0$  of minimum sound velocity ( $\varphi=90^\circ$ ,  $\theta=115^\circ$ ) and the expectation of the end of § 2 is verified by numerical computation. The amplification coefficient  $\alpha$  has a strong maximum along the direction  $\varphi=90^\circ$ ,  $\theta=113^\circ \pm 4^\circ$ . This

direction and those deduced by symmetry are shown in Fig. 1. If off-axis amplification is assumed in the above direction, we must observe a transverse acoustoelectric field along [001], zero field along [100] and a critical drift velocity given

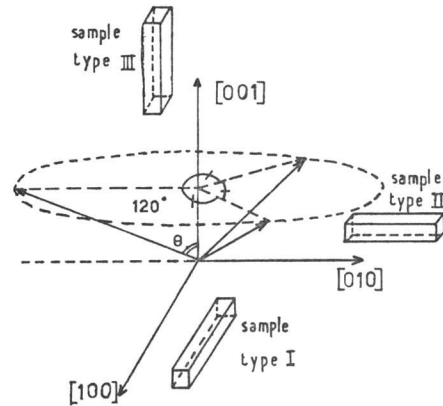


Fig. 1. Directions of maximum amplification.

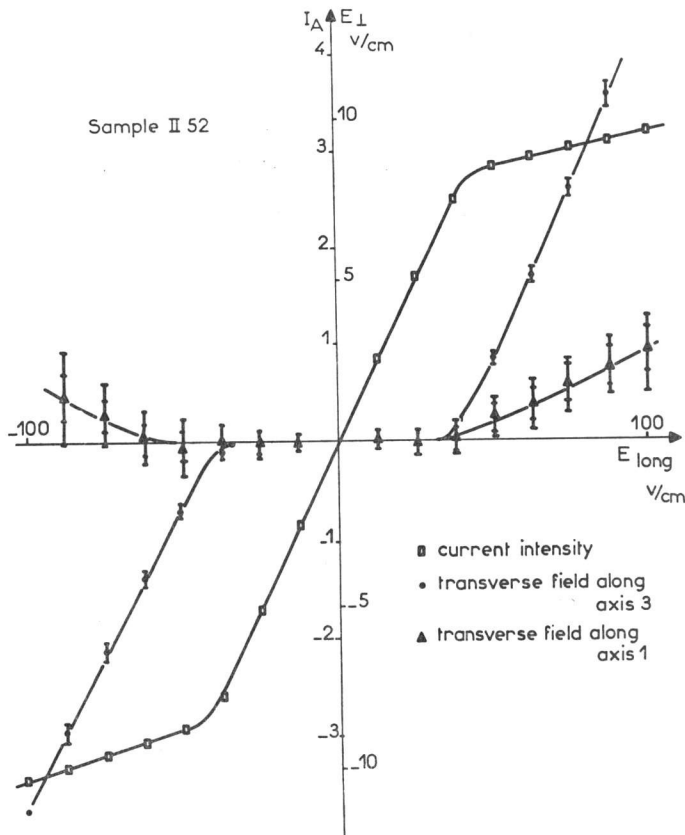


Fig. 2. Variations of current intensity and transverse field with the longitudinal field.

by  $\mu_H E_c = (1.14 \pm .02) \times 10^5$  cm/sec.

The agreement with experiments is rather good (see Table I). For a wave propagating along [010] we would find  $V_{s2} = 1.48 \times 10^5$  cm/sec. A high field domain trapped near a defect was observed on sample II 52.

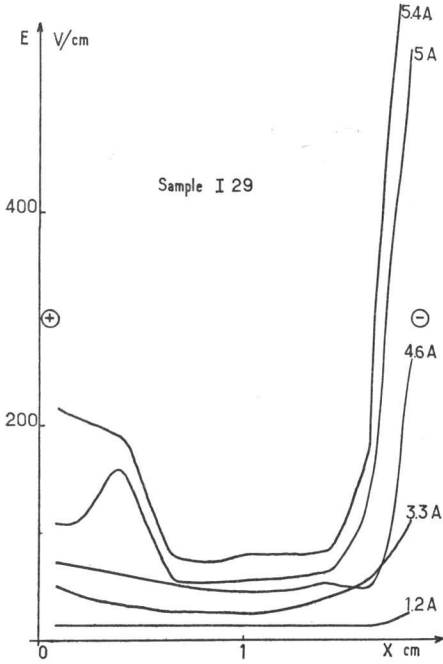


Fig. 3. Electric field repartition.

When the longitudinal field exceeds the critical value we observe a transverse field, the amplitude of which is at least 5 times smaller along [100] than along [001] (Fig. 2).

c) Type I samples (axis along [100])

The calculated direction of maximum  $\alpha$  is in

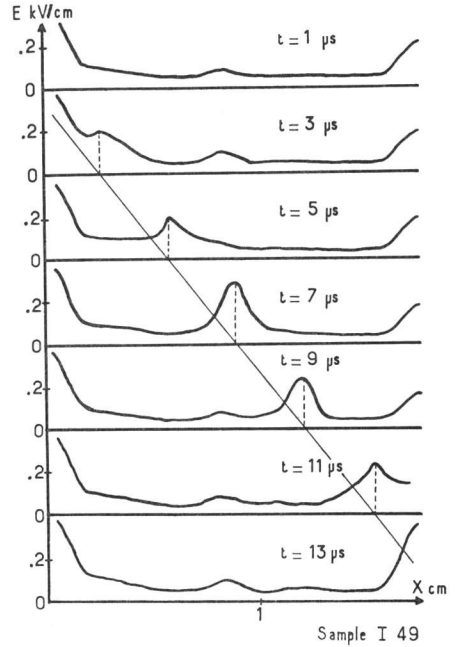


Fig. 4. Motion of high field domain.

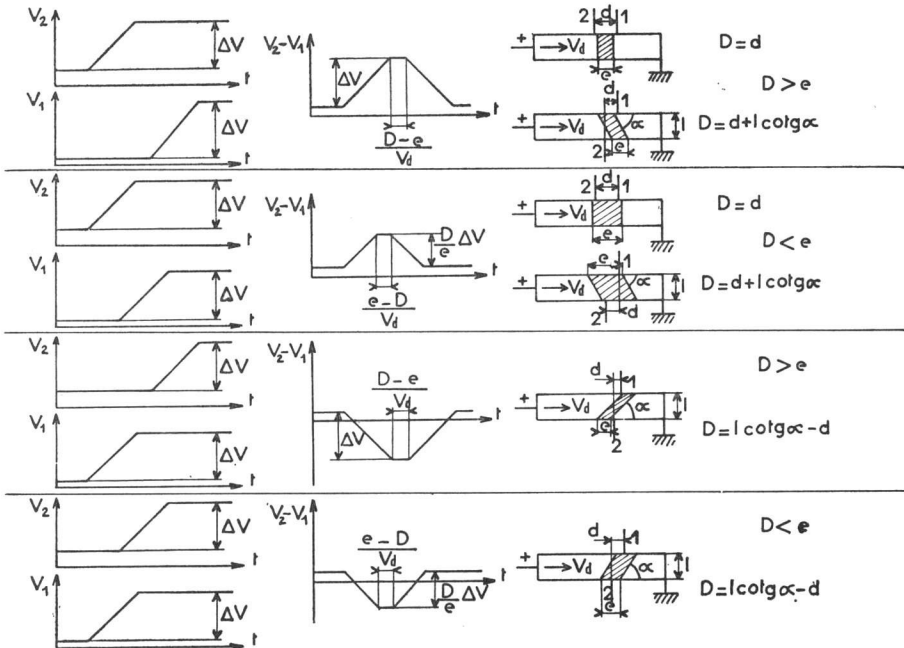


Fig. 5. Voltage variations for tilted domain.

the plane (010) and two other planes deduced by symmetry (Fig. 1). One of these directions is perpendicular to the sample axis and the two others are ( $\varphi=30^\circ$ ,  $\theta=72^\circ\pm6^\circ$ ) and ( $\varphi=30^\circ$ ,  $\theta=108^\circ\pm6^\circ$ ). These directions are symmetrical about [100] and give the same value of  $\alpha$  and an electroacoustic field along [100], but any defect or misorientation of crystal can make one of the  $\alpha$  greater and explains the occurrence of a transverse field.

Both "trapped" and moving domains were observed on these samples (Figs. 3 and 4). For "trapped" domains, the field can reach 600 V/cm and we observe a transverse field. The theoretical and experimental values of  $E_{\perp 2}/E_{\perp 3}$ , relation between transverse field along [010] and [001] are

$$(E_{\perp 2}/E_{\perp 3})_{\text{exp}}=1.8, (E_{\perp 2}/E_{\perp 3})_{\text{th}}=1.7\pm.5.$$

The incubation time of moving domains is about 1  $\mu$ s, its width is about 1 mm; the field inside it is several hundred V/cm. In Table I,  $V_d$  is the domain velocity along [100]. It agrees very well with the theoretical value  $V_{\text{th}}=(1.35\pm.05)\times 10^5$  cm/sec. For a wave propagating along [100] we would find  $2.41\times 10^5$  cm/sec. On sample I 49 which exhibited current oscillations, we used transverse probes and observed the propagation of a tilted domain. The possible potential differences observed for a tilted domain are discussed in Fig. 5; any change of the sign of this

difference occurring between transverse probes without the same phenomenon between longitudinal ones is only possible in the two later configurations. We assumed for simplicity of drawing a domain of constant field. The angles between the domain and the crystal axis are deduced from the width, the amplitude and the polarity of the peaks observed between different probes. The deduction of the normal to plane of the domain is found to be  $\varphi=28^\circ\pm6^\circ$ ,  $\theta=71^\circ\pm3^\circ$ , and is the same as the direction of maximum amplification given above within the limits of error.

### References

- 1) G. Quentin and J. M. Thuillier: *Proc. Int. Conf. Semiconductor Physics*, Paris (1964) p. 571.
- 2) T. Ishiguro, A. Hotta and T. Tanaka: *Japan J. appl. Phys.* **5** (1966) 335.
- 3) G. Quentin and J. M. Thuillier: *Phys. Letters* **19** (1966) 631.
- 4) G. Quentin and J. M. Thuillier: *Solid State Commun.* **4** (1966) 3.
- 5) A. R. Hutson and D. L. White: *J. appl. Phys.* **33** (1962) 40.
- 6) D. L. White: *J. appl. Phys.* **33** (1962) 2547.
- 7) Note: The tensor  $\vec{c}$  does not respect the symmetry of crystal class because we work neither with constant  $\vec{E}$  nor with constant  $\vec{D}$ .
- 8) Y. Kanai: *J. Phys. Soc. Japan* **14** (1959) 1118.

### DISCUSSION

**Kalashnikov, S.C.:** The small inhomogeneities may have strong influence on the domain motion. An electrode has such an inhomogeneity. Were there some differences in surface (contact) layers resistivity for two kinds of your samples (with immobile and with moving domains)?

**Quentin, G.:** In samples with "Trapped" domain greater inhomogeneities of resistivity are present than in samples with moving domains but the mean resistivity of the material is the same in the two kinds of samples.